JOURNAL OF GEOPHYSICAL RESEARCH, VOL. 112, D06213, doi:10.1029/2006JD007348, 2007

Aerosol radiative forcing efficiency in the UV region over southeastern Mediterranean: VELETA2002 campaign

A. M. Díaz,[1] O. E. García,[1] J. P. Díaz,[1] F. J. Expósito,[1] M. P. Utrillas,[2] J. A. Martínez-Lozano,[2] L. Alados-Arboledas,[3] F. J. Olmo,[3] J. Lorente,[4] V. Cachorro,[5] H. Horvath,[6] A. Labajo,[7] M. Sorribas,[8] J. M. Vilaplana,[8] A. M. Silva,[9] T. Elias,[9] M. Pujadas,[10] J. A. Rodrigues,[11] and J. A. González[12]

Received 29 March 2006; revised 4 October 2006; accepted 24 October 2006; published 31 March 2007.

[1] Atmospheric aerosol effects on spectral global UV irradiance were evaluated during the VELETA2002 field campaign between 8 and 19 July 2002 in southeast Spain. In the first stage, seven UV spectroradiometer and six CIMEL Sun photometer measurements were carried out simultaneously, allowing them to be calibrated and intercompared. The mean ratio obtained for the global irradiance between the spectroradiometers, with regards to a reference instrument, ranges from 0.98 up to 1.04 with standard deviations that oscillate between ±0.01 and ±0.17. In particular, the two spectroradiometers used to obtain the aerosol forcing efficiencies have a ratio of 1.000 ± 0.001. The aerosol optical depth (AOD) obtained with the CIMEL Sun photometers has a standard deviation of lower than ±0.01 for all the channels. Under clear sky conditions, the diurnal aerosol forcing efficiency (ΔDF_e) and fractional diurnal forcing efficiency (ΔFDF_e) was calculated for two Mediterranean stations: Armilla (691 m.a.s.l.) within the boundary layer and Sabinas (2200 m.a.s.l) on the lower limit of the free troposphere and 25 km away from the first station. The ΔDF_e values obtained at Armilla range between -2.72 ± 0.45 W m$^{-2}/\tau_{380}$ and -2.88 ± 0.45 W m$^{-2}/\tau_{440}$ and between -3.22 ± 0.61 W m$^{-2}/\tau_{380}$ and -3.40 ± 0.62 W m$^{-2}/\tau_{440}$ at Sabinas station; the ΔFDF_e values range from $-8.0 \pm 1.4\%/\tau_{380}$ to $-8.6 \pm 1.3\%/\tau_{440}$ and $-12.0 \pm 2.3\%/\tau_{380}$ to $-12.6 \pm 2.3\%/\tau_{440}$ at the two stations, respectively. Also, an experimental aerosol transmittance factor, C_T, used to obtain UV satellite derived products was found as a result of the dependence of the global irradiance with the AOD, under cloudless conditions. The average aerosol attenuation factor, η, obtained from the C_T, is 6 ± 2% under weakly absorbing aerosols, with a negligible spectral dependence.

Citation: Díaz, A. M., et al. (2007), Aerosol radiative forcing efficiency in the UV region over southeastern Mediterranean: VELETA2002 campaign, *J. Geophys. Res.*, *112*, D06213, doi:10.1029/2006JD007348.

1. Introduction

[2] Increases in UV levels are harmful to human health producing blindness or skin cancer; The United Nations Environment Programme [*World Health Organization*, 1994] has estimated that over 2 million nonmelanoma skin cancers and 200,000 malignant melanomas occur globally each year. Further, the impact of increasing UV levels over many biological processes such as crop production, photosynthesis, aquatic ecosystems, etc., is largely unknown. Essential therefore are the ground based and satellite measurements that allow us to determine the amount and also the trends of UV irradiance at the surface. From ground based instruments the improvement of data quality has been the main goal in recent years establishing quality control (QC) and quality assurance (QA) programmes such as QASUME [*Gröbner et al.*, 2004]. Even though the absolute accuracy of individual instruments using diverse calibration methods can be considered sufficient, intercomparison between the instruments is an important way to provide uniform data

[1]Departamento de Física, Universidad de la Laguna, Tenerife, Spain.
[2]Grupo de Radiación Solar, Universitat de València, València, Spain.
[3]Grupo de Física de la Atmósfera, Universidad de Granada, Granada, Spain.
[4]Departamento de Astronomía i Meteorología, Universitat de Barcelona, Barcelona, Spain.
[5]Grupo de Óptica Atmosférica, Universidad de Valladolid, Valladolid, Spain.
[6]Experimental Physics Institute, University of Vienna, Vienna, Austria.
[7]Instituto Nacional de Meteorología, Madrid, Spain.
[8]Estacion de Sondeos Atmosféricos de El Arenosillo, Instituto Nacional de Técnica Aeroespacial, Huelva, Spain.
[9]Évora Geophysics Centre, University of Évora, Évora, Portugal.
[10]Departamento de Impacto Ambiental de la Energía, Centro de Investigaciones Energéticas, Medioambientales y Tecnológicas, Madrid, Spain.
[11]Instituto Superior Tecnico of Lisbon, Lisbon, Portugal.
[12]Departamento de Física, Universitat de Girona, Girona, Spain.

0148-0227/07/2006JD007348

Table 1. Spectroradiometers Participating in VELETA 2002

Instrument	Institution	Detector	Optical Input	Temperature Control	FWHM, nm	Wavelength Range, nm	Wavelength Correction	Dark Current Correction	Station	Period, days of July
Brewer MK III	INTA (Instituto Nacional de Técnica Aerospacial) El Arenosillo (ARB)	Photomultiplier EMI 9789QA	quartz dome	no	0.62	290–363	yes	yes	Armilla	10–19
Bentham DM150	University of Granada (UGR)	Photomultiplier R1527	Teflon diffuser	yes	1.18	250–650	yes	yes	Armilla Sabinas	10–12, 13–20
Bentham DM150	University of Barcelona (UBB)	Fotomultiplicador DH10(Bi)	Teflon diffuser	yes	1.35	285–400	yes	yes	Armilla Veleta	10–12, 13–19
Optronic 754	University of Valencia (UVO)	Photomultiplier S–20	integrated sphere	no	1.60	300–700	yes	yes	Armilla	10–18
Optronic 752	University of La Laguna (ULL)	Photomultiplier S–20	Teflon diffuser	yes	1.10	290–700	yes	yes	Armilla Motril	10–12, 13–18
Oriel MS257	University of Girona (UGI)	Photomultiplier SI70336	integrated sphere	no	1.80	300–980	yes	yes	Armilla Pitres	10–12, 13–18
Macam SR9910	University of La Rioja (URM)	Photomultiplier S–20	integrated sphere	no	1.90	240–800	yes	yes	Armilla	10–12

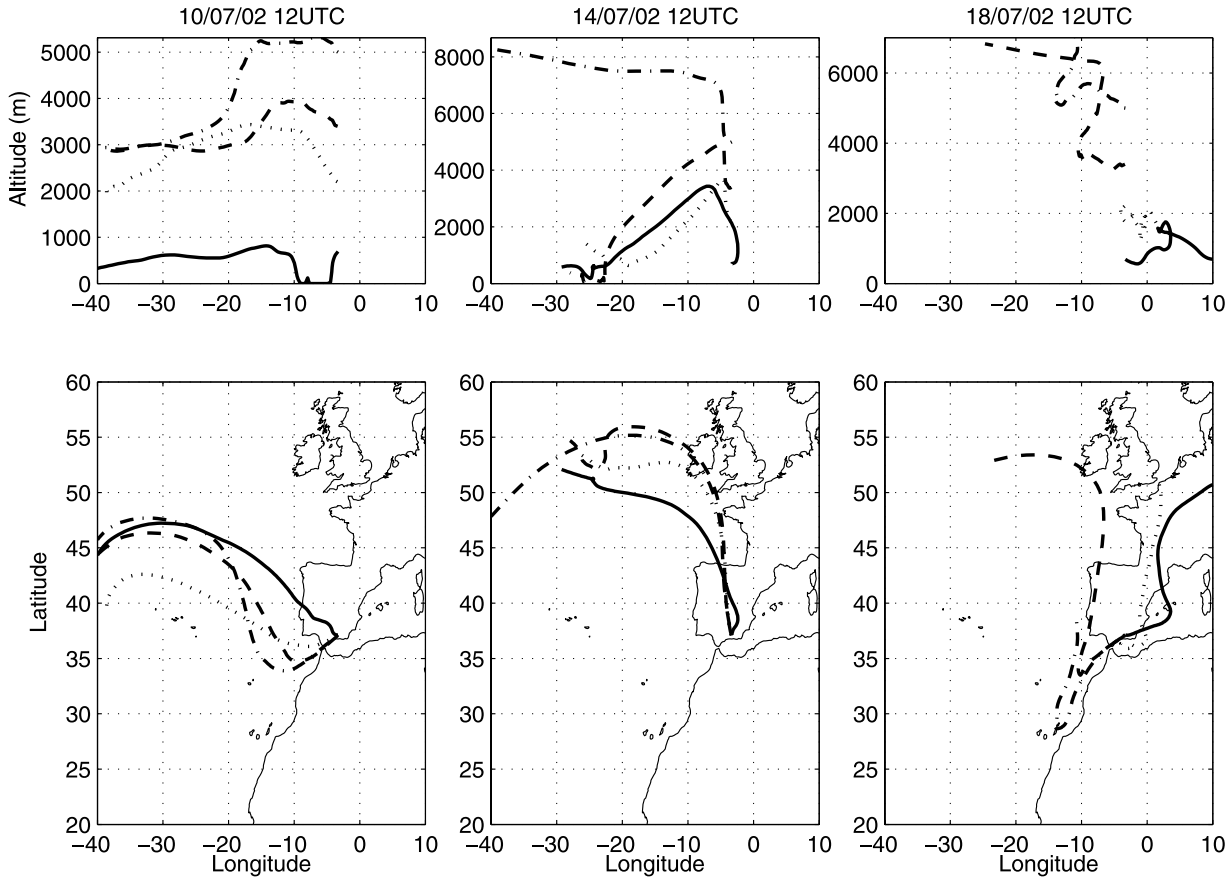

Figure 1. Five days isentropic back trajectories calculated over Armilla station at four different altitudes: 691, 2200, 3398 and 5000 m.a.s.l at 1200 UTC.

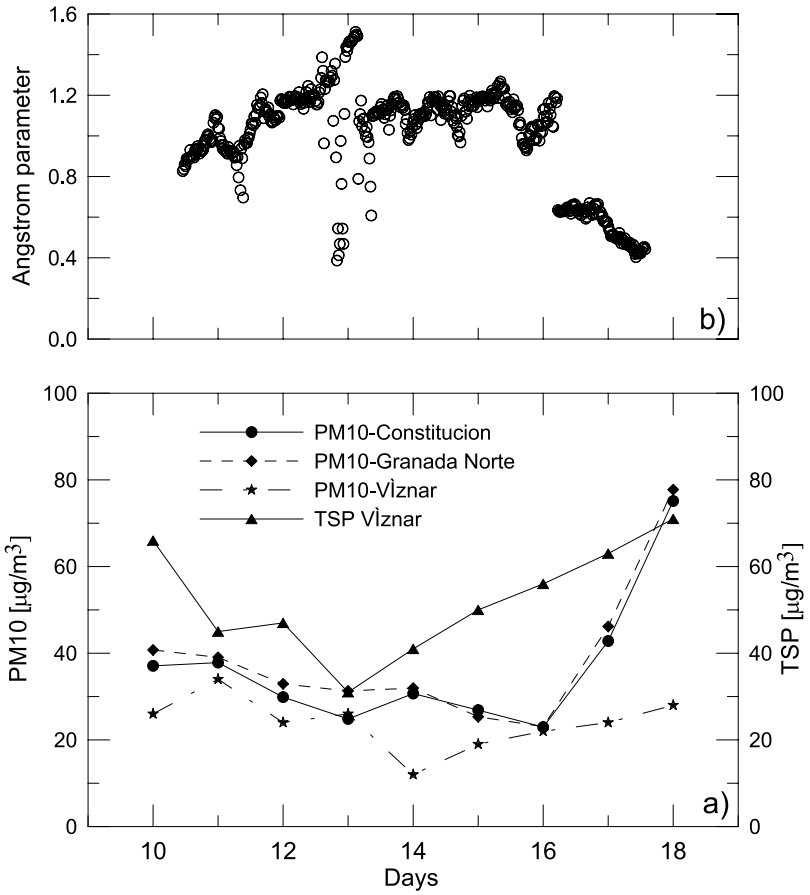

Figure 2. (a) PM10 values for two urban and one background EMEP stations: Constitución P.F. (37.19°N 3.62°W) and Granada Norte (37.19°N 3.61°W), Viznar (37.24°N 3.47°W) (left axis) and TSP values only for the background station Viznar (right axis). These stations are located in the area of Granada and the measurements correspond to the period of the campaign. (b) Angstrom parameter obtained from the CIMEL measurements in Armilla station.

quality. With regards to satellite instruments they measure radiometric variables and use radiative transfer models to calculate surface UV irradiance on a global scale. Under cloud-free conditions the accuracy of satellite UV data is limited mainly by the knowledge of the highly variable aerosol properties [*World Meteorological Organization* (*WMO*), 2003; *Krotkov et al.*, 1998]. Thus the effect of aerosols on satellite UV estimation over large areas is greater in tropical regions where the largest dust (e.g., the Saharan plume) and smoke plumes (e.g., Africa and South America, as a result of biomass burning) are found. In these regions the reductions in surface UV irradiance are frequently as much as 50% [*Herman et al.*, 1999].

[3] They *Intergovernmental Panel on Climate Change* [2001] also evidenced that although the estimated radiative forcing by the main greenhouse gases is relatively well understood, that is not true in the estimation of direct and indirect radiative forcing by aerosols because of its high uncertainty. Recent studies into radiative forcing have focused mainly on the visible part of the spectrum. For instance, *Jayaraman et al.* [1998] found that direct solar flux in the visible spectrum decreased by 42 ± 4 W m^{-2} and diffuse sky radiation increased by approximately 30 ± 3 W m^{-2} with every 0.1 increase in aerosol optical depth at 497 nm for solar zenith angles smaller than 60° at the surface. *Rajev and Ramanathan* [2001] showed that the observed TOA clear sky aerosol forcing varied between -4 and -14 W m^{-2} in the Northern Hemisphere and between 0 and -6 W m^{-2} in the Southern Hemisphere. *Díaz et al.* [2001] obtained mineral dust radiative forcing values of -1.22 W m^{-2} over oceans and -0.57 W m^{-2} over continents, on a global scale. Recently, *Hatzianastassiou et al.* [2004] found that under clear skies, on a mean annual and global-scale aerosols decrease the solar radiation reaching the Earth's surface by 1.9 W m^{-2}.

[4] Therefore the main objective of this study is to determinate the aerosol radiative forcing efficiency at UV wavelength. First in section 2, the quality assessment and quality control of the UV global irradiance and aerosol optical depth measurements were carried out. In this section the site and instrumentation along with the spectroradiometers and Sun photometers calibration and intercomparison results obtained during VELETA2002 field campaign were presented. Next in section 3 forcing efficiency at the surface

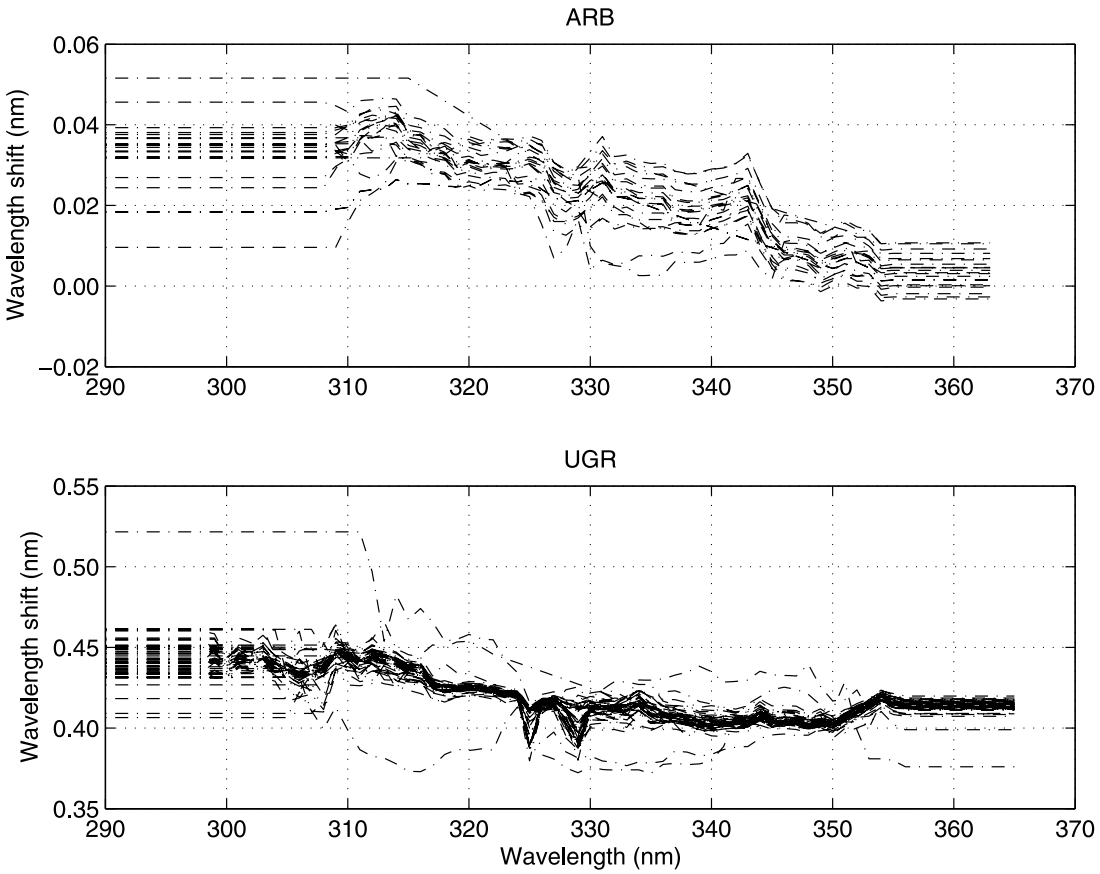

Figure 3. Wavelength shifts for the spectroradiometers ARB and UGR calculated by Slaper method. The different curves correspond to different scans made every half an hour.

was calculated and the transmittance factor (C_T) used to estimate the UV irradiance at the surface by satellite under aerosol presence was experimentally evaluated.

2. UV Spectral Irradiance and Aerosol Optical Depth Measurements

2.1. Site and Instruments Description

[5] The VELETA2002 field campaign took place in Granada (37.11°N 3.35°W), Spain, between 8 and 19 July 2002. The campaign was designed to allow the evaluation of atmospheric aerosols effects on UV irradiance at different altitudes; from sea level up to 3398 m.a.s.l. [*Alados-Arboledas et al.*, 2004]. In the first week of the campaign, an intercomparison of the different instruments was carried out in order to assess the quality of the measurements. Among the participant instruments in this campaign we are going to focus particularly on the spectroradiometers (used to measure UV spectral surface downwelling irradiances) and the Sun photometers (used to calculate Aerosol Optical Depth, AOD). The main characteristics of these instruments are summarized in Table 1, as well as their spectral measurement ranges. The CIMEL Sun photometers are standard Sun/sky photometer from the AERONET network that operates automatically [*Holben et al.*, 1998] (see http://aeronet.gsfc.nasa.gov/). One of the CIMEL participants (#109) is an AERONET instrument which belongs to the National Aeronautic and Space Administration (NASA).

[6] The two stations selected for this study were: Armilla station (37.13°N 3.32°W, 691 m.a.s.l.), located within the boundary layer, at which the instrument intercomparison took place. This station is located 8 km away from the city of Granada and is surrounded by crops, influenced by urban aerosol and eventually by biomass burning. The presence of Saharan dust at this location is also possible because of its proximity to North Africa. Sabinas station (37.12°N 3.43°W, 2200 m.a.s.l.) is located in the lower limit of the free troposphere according to the LIDAR measurements (data not shown). This station also being located close to the city of Granada can be influenced by urban aerosol. In both stations one spectroradiometer and one CIMEL Sun photometer were placed: in particular at Armilla, the Brewer ARB and the CIMEL #394, and in Sabinas, the Bentham UGR and the CIMEL #307. In addition, at both sites, other ancillary instrumentation can be found such as the YANKEE UVB−1 radiometer, LICOR spectroradiometers that measure global and direct irradiance from the UV to IR regions, a telephotometer used to measure the horizontal extinction at given wavelengths and finally temperature and humidity sensors.

[7] The synoptic situation during the first days of the campaign was governed by the Azores high-pressure system which produces wind from the north-northwest over the Iberian Peninsula. However, this meteorological pattern changed over 17 to 20 July where a thermal low developed over the Peninsula bringing air masses to the stations from

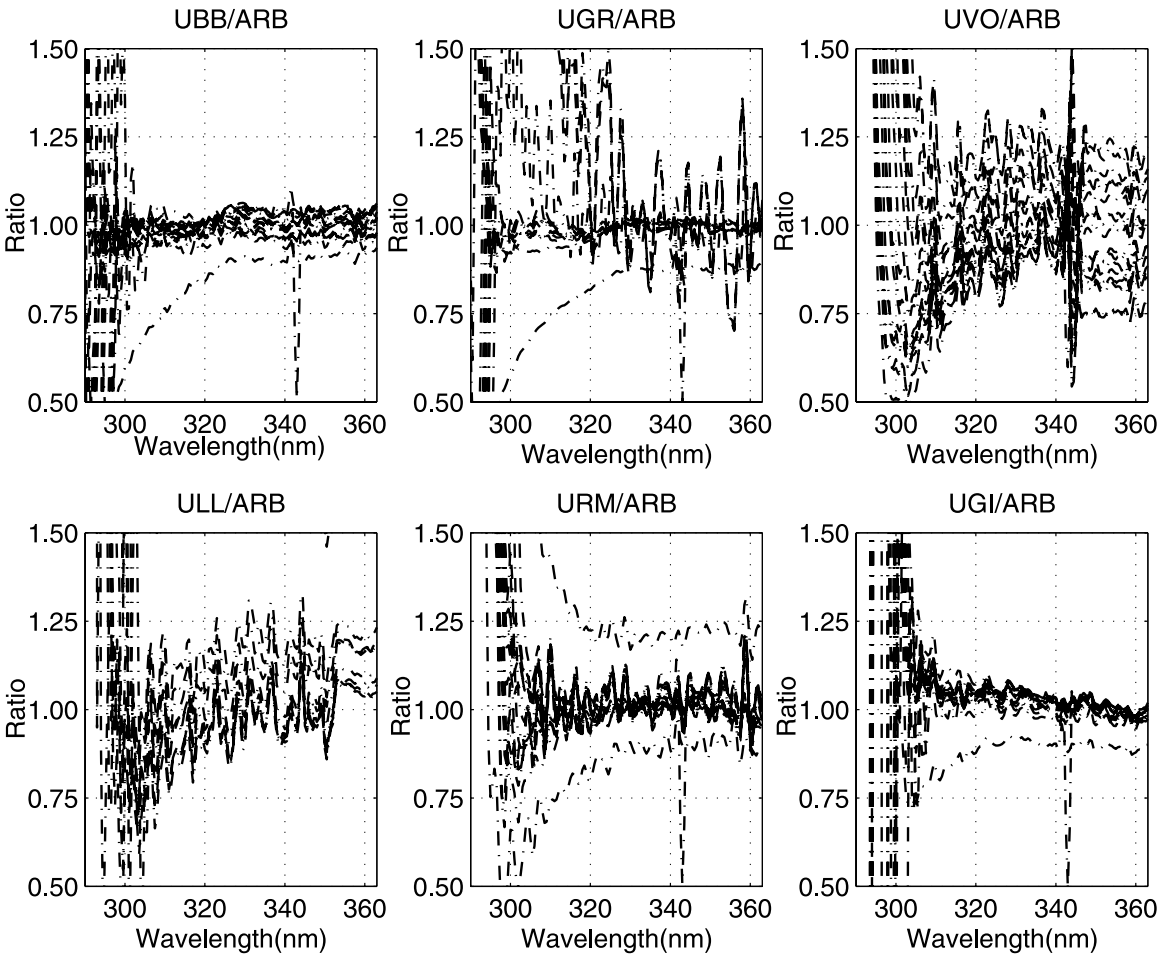

Figure 4. Ratios of global UV irradiance for all spectroradiometers participating in VELETA2002 campaign. The Brewer ARB was used as the reference instrument. The different curves correspond to the measurements made every half an hour during 10 July 2002 (day of intercomparison 191).

the Mediterranean Sea. Figure 1 shows the representative isentropic back-trajectories calculated over 5 days at four different altitudes: 691, 2200, 3398 and 5000 m over Armilla station. These back trajectories were calculated daily with HYSPLIT4 [*Draxler and Hess*, 1997] model at 1200 UTC. During the first 4 days of the campaign (10–13 July) the trajectories show air masses from the North Atlantic Ocean at all altitudes. This situation changed between 14 and 17 July because of the arrival of air masses from the north of the Peninsula. From 18 July to the end of the campaign, 20 July the situation changed again with air masses from the Mediterranean Sea arriving from the African coast. PM10 data from three European Monitoring Evaluation Programme (EMEP) stations are shown in Figure 2a along with the Angstrom parameter, Figure 2b. Two of these stations are urban: Constitución P.F. and Granada Norte; the third being a rural background station, Viznar, located at 1230 m.a.s.l and being located 9 km away from Granada city. The PM10 concentration during the campaign was less than 40 $\mu g/m^3$, which is the standard value in this area (http://www.emep.int/), but increased on 18 July when the synoptic situation changed bringing air masses from the African continent. The TSP (Total Suspended Particles) values registered at Viznar, which are also shown, follow the same behavioral pattern.

2.2. Spectroradiometer Calibration and Intercomparison

[8] In order to evaluate the effects of UV radiation (0.2–0.4 μm) it is essential to obtain reliable measurements of

Table 2. Statistics of the Spectral Global Irradiance Ratios Between Each Instrument and the Reference: Mean, Mean Absolute Deviation, MAD, Mean Bias Deviation, MBD and Root Mean Square Deviation, RMSD, During the Intercomparison Days[a]

Equipment	Mean Ratio	MAD	MBD	RMSD
UBB	1.000	0.023	0.001	0.028
UGR	**1.000**	**0.010**	**0.002**	**0.010**
UVO	0.978	0.140	0.022	0.165
ULL	1.027	0.113	0.027	0.146
UGI	1.000	0.070	0.002	0.130
URM	1.040	0.080	0.040	0.120

[a]Boldface indicates the spectroradiometer used jointly with the reference instrument to obtain the forcing efficiency.

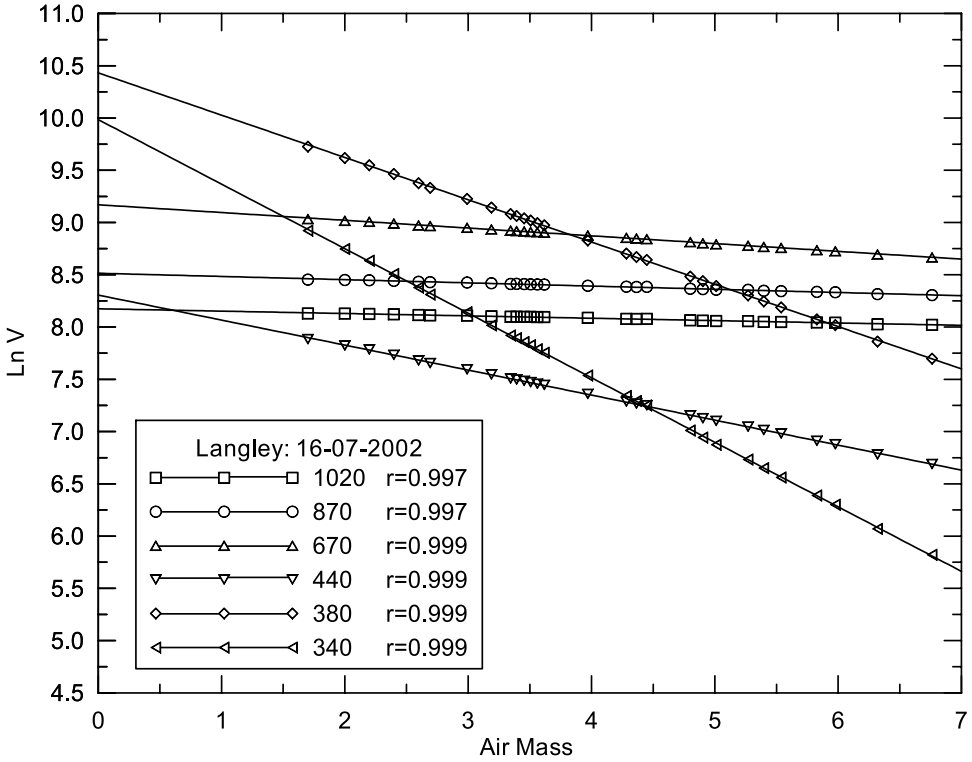

Figure 5. Langley plot for the CIMEL #307 during the morning of 16 July.

spectral irradiance. UV measurements gathered at different times and places must be expressed on an absolute scale of irradiance in order to be related to each other. The most widely used method to transfer the calibration involves the use of spectral irradiance lamps. In this campaign, new portable lamps of 150 Watt traceable NIST (National Institute of Standards and Technology) were used to calibrate the instruments, the spectroradiometers therefore measured all the lamps available and compatible with its optical input. Moreover, each instrument also measured a mercury lamp in order to correct the wavelength misalignment as well as to obtain the slit function and the Full Width at Half Maximum value (FWHM). With this methodology we can evaluate the relative differences between the instruments which are essential in this study. One of the most important factors to take into account in the calibration process is the current that passes through the filament of the lamp. Note that for a 1000 Watt FEL lamp, an error of 1% in the current produces an error of 10% in the spectral irradiance at the wavelength of 300 nm [*Gardiner and Martin*, 1997]. This current must therefore be controlled with a high degree of accuracy during the whole process and maintained at the same value that was used to calibrate the lamp. Despite the power supply used in this campaign to keep the current constant, an electronic system composed of a high-precision resistor with a value of $0.010130 \pm 0.000001\ \Omega$, and a 6 digit voltmeter were employed to test the efficiency of this control. The last two instruments were calibrated before the campaign.

[9] The accuracy of the calibration factors obtained under this methodology was tested during the intercomparison between instruments. This intercomparison is necessary as to determine the relative differences between instruments, thus assuring that the variations in the irradiance levels are solely due to the altitude and/or the aerosol effects. The instruments measured global and diffuse spectral irradiance simultaneously every 15 min during the days 191 and 192 (10 July 2002 and 11 July 2002). The spectral range goes from 290 to 365 nm with 0.5 nm intervals, and for those instruments that can measure in the VIS–IR region, 370 to 800 nm, every 5 nm. The temporal interval between wavelengths was 3 s.

[10] To determine the wavelength shift of each instrument, the technique developed by *Slaper et al.* [1995] and *Slaper and Koskela* [1997] on the basis of the detection of Fraunhofer lines in order to align the spectral measurements was applied. Figure 3 shows as an example of the wavelength shift for the Brewer ARB and the Bentham UGR. It has to be mentioned however, that even if the spectral measurements were perfectly aligned, the differences in the slit functions of the instruments would still cause scatter in their ratios. It is necessary therefore to deconvolve the data using the specific slit function of each instrument and to perform then a convolution using a common slit

Table 3. Retrieved Calibration Coefficients and Standard Error of the Mean for the CIMEL #307

Wavelength, nm	V_0, a.u	Standard Error	% Error
1020	3526.47	19.56	0.55
870	4936.30	25.72	0.52
670	9508.00	37.51	0.39
440	3971.52	27.83	0.70
380	33057.31	329.16	1.00
340	21024.29	244.46	1.16

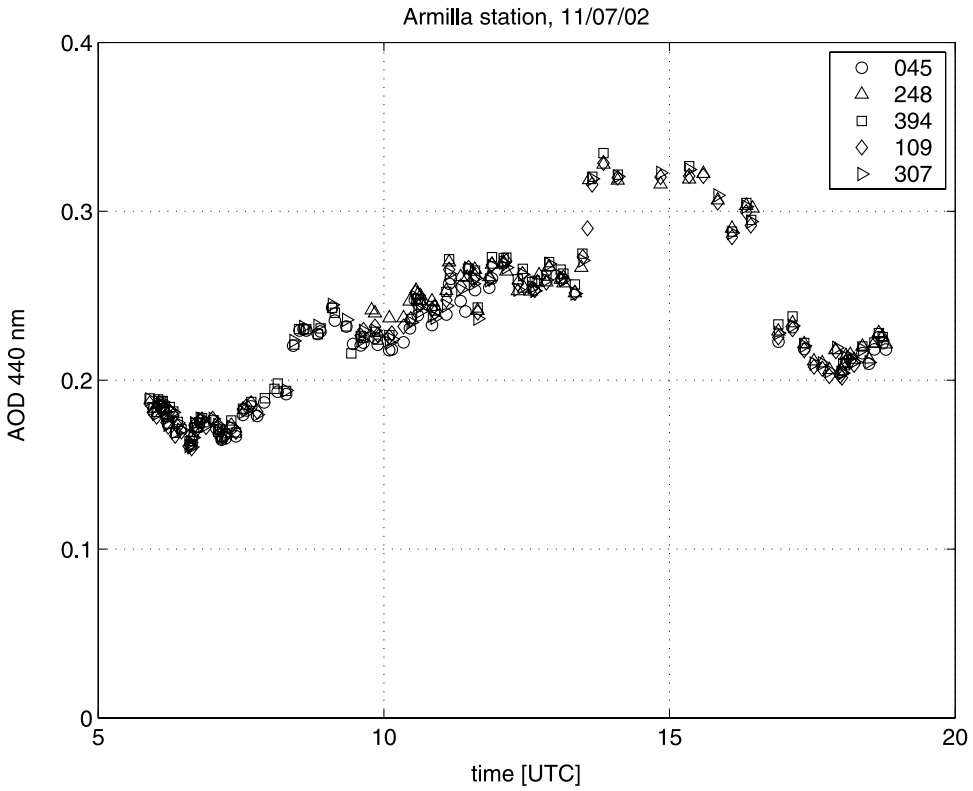

Figure 6. Comparison of the evolution of AOD along day 11 July at Armilla, obtained with a common methodology and calibration source.

function; in our case, this common slit function has a FWHM of 1 nm.

[11] On the basis of the stability of the calibration factors evaluated previously during and after the campaign, and also the small wavelength shift of less than 0.05 nm, the Brewer from INTA (Instituto Nacional de Técnica Aeroespacial), ARB, was selected as the reference instrument in this campaign. In order to evaluate the variation between the spectroradiometers with regards to the reference instrument the following statistical parameters were calculated: mean, mean bias deviation (MBD), mean absolute deviation (MAD) and the root mean square deviation (RMSD). The ratios were then evaluated as wavelength and time functions. The ratios as a function of wavelength are shown in Figure 4 whereas the associated statistical parameters are presented in Table 2.

[12] The two spectroradiometers selected to evaluate the differences in the spectral global UV irradiance during the second week of the campaign were the reference instrument Brewer ARB, and the Bentham UGR, with a mean ratio of 1.000 and the smallest standard deviation 0.001.

2.3. Calibration and Intercomparison of CIMEL Sun Photometers

[13] The Sun photometers were calibrated according to the standard procedure for Langley plots during mornings from 8 to 11 July in a station located at 2103 m.a.s.l. The CIMEL #307 measured during 14 days of this campaign in a station located at high altitude (2200 m.a.s.l.), recording Langley calibrations with high quality and correlation coefficients for all channels close to 0.999 (Figure 5). From all the measurements made by this Sun photometer the more stable mornings were used to obtain its calibration coefficients, these being referenced in Table 3 along with their standard errors. These calibration coefficients were compared with those provided by the AERONET NASA CIMEL, #109, presenting a deviation of less than 1% in almost all wavelengths with two exceptions: 340 nm with a deviation of 3.8% and 670 nm with a deviation of 1.6% (data not shown). Taking into account however, that the nominal uncertainty for the calibration coefficients from AERONET field instruments is around 1–2% [*Holben et al.*, 1998; *Eck et al.*, 1999], this last calibration is still

Table 4. Root Mean Square Deviation, RMSD, Mean Bias Deviation, MBD, and Standard Deviation, STD, of AOD From AERONET and GFAT2 CIMEL Regarding the GAFT1 CIMEL #307 When the Common Methodology Is Applied

AERONET #109				GFAT2 #394			
λ, nm	RMSD	MBD	STD	λ, nm	RMSD	MBD	STD
340	0.009	0.008	0.005	340	0.24	0.024	0.24
380	0.008	0.007	0.004	380	0.010	−0.001	0.010
440	0.003	0.000	0.003	440	0.009	−0.003	0.008
670	0.008	−0.006	0.005	670	0.011	−0.007	0.009
870	0.004	−0.001	0.003	870	0.007	−0.003	0.006
1020	0.006	0.001	0.006	1020	0.012	−0.003	0.012

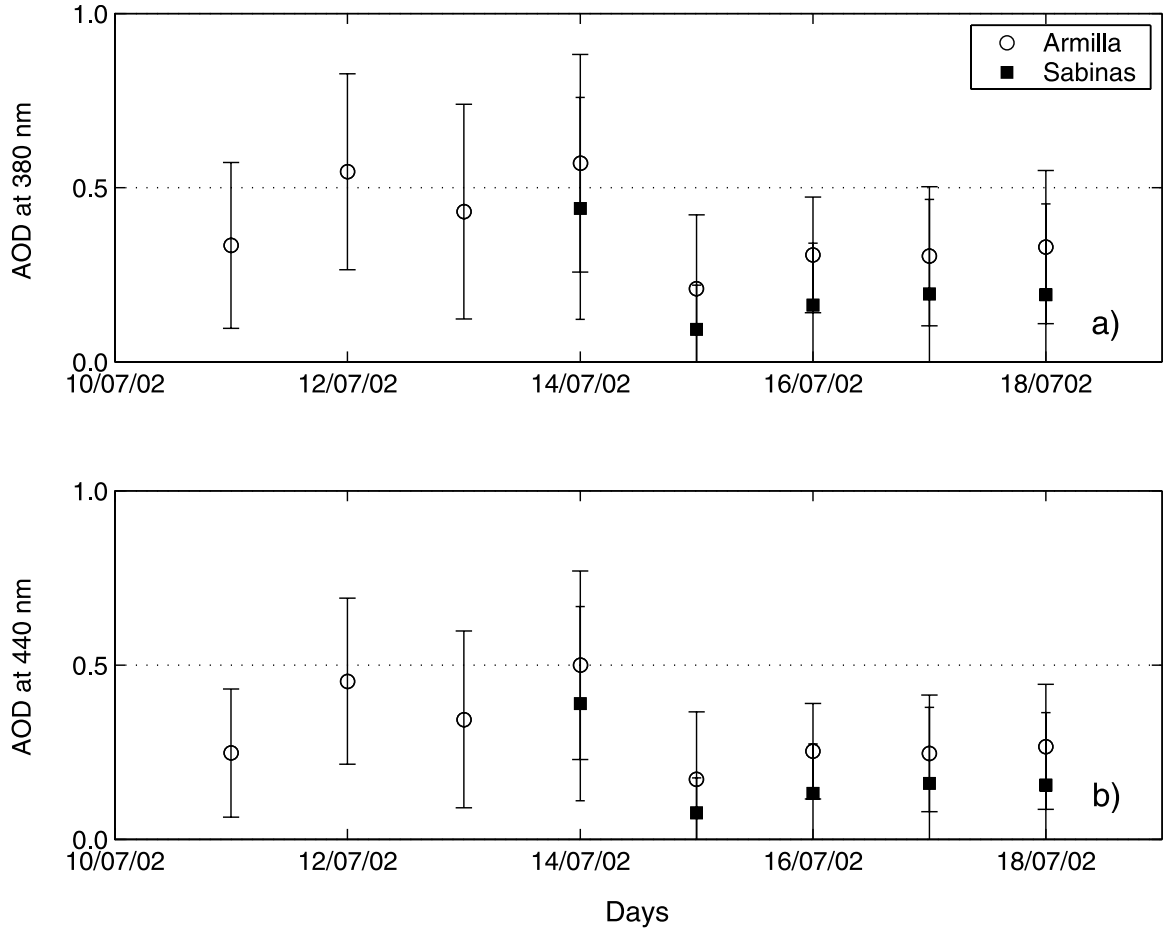

Figure 7. Daily mean AOD values at Armilla and Sabinas stations at (a) 380 nm and (b) 440 nm.

consistent with that provide by AERONET, with the exception of the channel at 340 nm.

[14] Once the CIMEL #307 was calibrated, the coefficients were transferred to the rest of the Sun photometers, making use of the simultaneous measurements obtained in the first week of the campaign. The criteria established in order to carry out the calibration transfer were: air masses of lower than 3.5; atmospheric stable conditions as to avoid rapid changes in the optical depth, and simultaneous measurements with less than 5 s of difference between each [*Estellés et al.*, 2006].

[15] The CIMEL intercomparison was made for the Aerosol Optical Depth, AOD, measurements. In order to reduce the uncertainties in the AOD comparison a common methodology was used by the different research groups described by *Estellés et al.* [2006]. Figure 6 shows the AOD values for 11 July when all Sun photometers were measuring simultaneously at Armilla station. To analyze this intercomparison three statistical parameters have been calculated: root mean square deviation, RMSD, mean bias deviation, MBD, and standard deviation STD. These three statistical parameters for the CIMEL #394 and #109 regarding to the CIMEL #307 are showed on Table 4. With reference to the AOD used to obtain the aerosol forcing efficiencies at 380 and 440 nm, the mean ratios between the CIMEL #307 and #394 were 1.00 ± 0.010 and 1.00 ± 0.008 respectively; and when compared with CIMEL #109 were 1.00 ± 0.004 at 380 nm and 1.00 ± 0.003 at 440 nm.

3. Aerosol Radiative Forcing Efficiency

[16] The forcing efficiency (ΔF_e) is defined as the irradiance variation per unit of aerosol optical depth [*Charlson et al.*, 1991]:

$$\Delta F_e = \Delta E / \Delta \tau \tag{1}$$

[17] The spectral irradiance was measured by two spectroradiometers: the Brewer MKIII (ARB), and the Bentham DM150 (UGR), described in 2.1. Each one of these instruments measured global spectral irradiance from sunrise to sunset, the ARB spectroradiometer every 30 min from 10 to 19 July and, the UGR instrument every 15 min from 13 to 19 July. With these different acquisition time resolutions we have 294 and 347 measurements respectively at Armilla and Sabinas stations. Clear sky conditions were determined from the fit to a Gauss function of the hourly irradiance measurements. A clear day is selected only if the determination coefficient is higher than 0.99. Under this criterion we have 9 and 5 days for Amilla and Sabinas respectively.

[18] The aerosol optical depth was measured in both stations by the CIMEL Sun photometers described in 2.1: #394 and #307 placed at Armilla and at Sabinas respec-

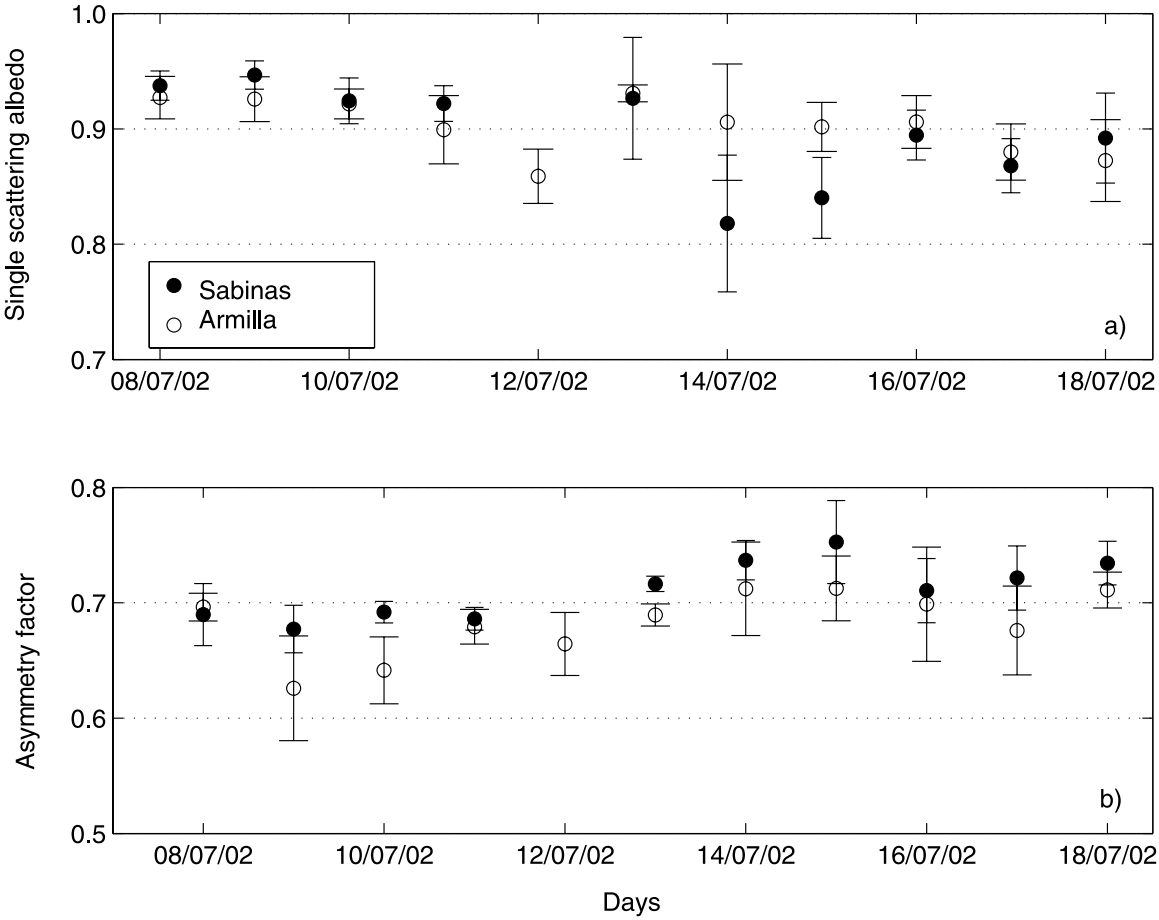

Figure 8. Daily mean values of (a) single scattering albedo and (b) asymmetry factor at 440 nm measured at Armilla and Sabinas stations during the campaign.

tively. Despite the fact that this instrument provides aerosol optical depth for a wide range of wavelengths ranging from 340 to 1020 nm, only 380 and 440 nm were selected as we are focusing on the UV region and the shortest wavelength, 340 nm, has an error of 3.8%. The AOD relative differences between the two CIMEL at the specified wavelengths are 1.00 ± 0.010 at 380 nm and 1.00 ± 0.008 at 440 nm. Daily AOD mean values at both stations are shown in Figures 7a and 7b at 440 and 380 nm respectively. These instruments also provide information about single scattering albedo (Figure 8a), asymmetry factor (Figure 8b) and Angstrom parameter (Figure 2b). The values of these last two parameters provide evidence the presence of absorbing aerosols over the stations. Moreover, Angstrom parameter and particle matter data (Figure 2) confirm clearly the arrival of Saharan dust on 18 July, where the concentration of particle matter increased considerably, and the Angstrom parameter reduced by up 0.5. However, not enough measurements were taken during the Saharan dust event to obtain the forcing efficiency, and so we are only going to focus on the days prior to this, from 10 to 17 July.

[19] Clear sky aerosol forcing efficiency, ΔF_e, is estimated using the slope method, and limited to solar zenith angles of less than 60° [*Jayaraman et al.*, 1998]. Thus hourly regression analysis between the integrated global irradiance within the range of 290–363 nm and also the AOD in the slant path at two different wavelengths: 380 and 440 nm were calculated in each station. The advantage of using this method is that we can avoid errors in simulating the clear day, i.e., without aerosols. Figure 9 shows these hourly forcing efficiencies obtained in Armilla and in Sabinas stations, from 10 a.m. to 3 p.m. The effectiveness of the method is demonstrated by the correlation coefficient which is higher than 90% in almost all cases. From these instantaneous forcing efficiencies (ΔF_e) a diurnal forcing efficiency (ΔDF_e) was calculated integrating these values from sunrise to sunset, averaging over a 24 hour period.

$$\Delta DF_e = \frac{1}{24}\int_{sunrise}^{sunset} \Delta F_e dt \tag{2}$$

[20] The ΔDF_e obtained values are: -2.72 ± 0.45 W m$^{-2}/\tau_{380}$ and -2.88 ± 0.45 W m$^{-2}/\tau_{440}$ in Armilla; and -3.22 ± 0.61 W m$^{-2}/\tau_{380}$ and -3.40 ± 0.62 W m$^{-2}/\tau_{440}$ in Sabinas station. These differences in the forcing efficiencies between both stations are mainly due to the AOD levels in Sabinas which are smaller than in Armilla. This behavior has been discussed by *Conant et al.* [2003], who pointed out that the aerosol forcing efficiency is modulated by the AOD; that is, aerosol forcing efficiencies are higher when AOD $\ll$ 1,

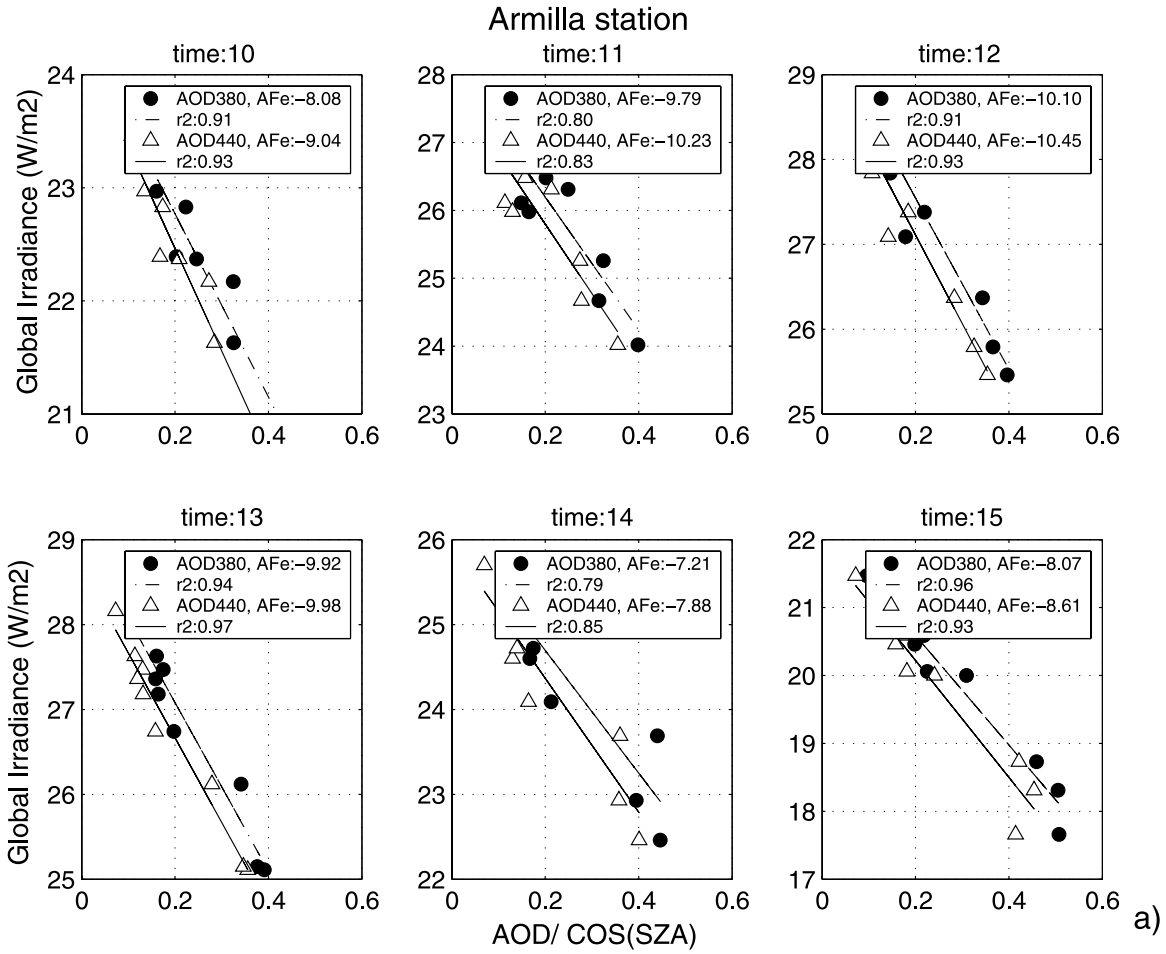

Figure 9. Hourly aerosol forcing efficiencies obtained at (a) Armilla and (b) Sabinas stations.

because of multiple-scattering effects and attenuation of the transmitted radiation.

[21] Another two useful magnitudes used to evaluate this radiative effect are the fractional forcing (FF) and the fractional forcing efficiency (FF_e) introduced by *Bush and Valero* [2003]. These parameters represent the percentage of incident solar radiation being forced by the atmosphere. In this study a fractional diurnal forcing efficiency, ΔFDF_e, has been calculated by taking the aerosol diurnal forcing efficiencies and dividing then by the TOA solar irradiance averaged over a 24 hour period.

$$\Delta FDF_e = \frac{\Delta DF_e}{\frac{1}{24}\int_{sunrise}^{sunset}(TOA)dt} \tag{3}$$

[22] The TOA irradiance integrated in the wavelength range of this study, 290–363 nm, is 57.74 W m^{-2} obtained from a high-resolution ATLAS-3 solar spectrum [*Van Hoosier*, 1996] and with an uncertainty in the absolute irradiances of 3%, for 15 July 2002. The fractional diurnal forcing efficiencies, ΔFDF_e, are: $-8.0 \pm 1.4\%/\tau_{380}$ and $-8.6 \pm 1.3\%/\tau_{440}$ in Armilla, and $-12.0 \pm 2.3\%/\tau_{380}$ and $-12.6 \pm 2.3\%/\tau_{440}$ in Sabinas.

[23] During the ACE–Asia experiment, *Bush and Valero* [2003] found for the visible spectral region at Gosan, diurnal forcing efficiency of -42.2 ± 4.8 W m^{-2}/τ_{500} and fractional diurnal forcing efficiency of $-26.7 \pm 3.3\%/\tau_{500}$. These results are not however readily comparable with those obtained in this study because of the different aerosol types, aerosol load and spectral ranges.

[24] Nevertheless, this campaign provides an excellent opportunity to evaluate the aerosol transmittance factor, C_T, under cloudless conditions. This magnitude being especially important for the aerosol corrections on the new UV surface irradiance products obtained by satellite such as Ozone Monitoring Instrument [*Krotkov et al.*, 2001; *Stammes and Noordhoek*, 2002]. This transmittance factor is defined by:

$$C_T = F_{aer}/F_{clear} \tag{4}$$

where F_{aer} and F_{clear} are the surface UV irradiance with and without aerosols presence respectively. *Kerr* [1997] found that the dependence of the aerosol transmittance factor, C_T, with the aerosol optical depth fitted to the expression:

$$C_T = e^{(-k\tau_\lambda)} \tag{5}$$

where the constant k lies in the range 0.2 to 0.3. *Krotkov et al.* [1998] examined this last factor for different aerosol models. They found k values for non absorbing aerosols of less than 0.15, for absorbing aerosols, this magnitude is

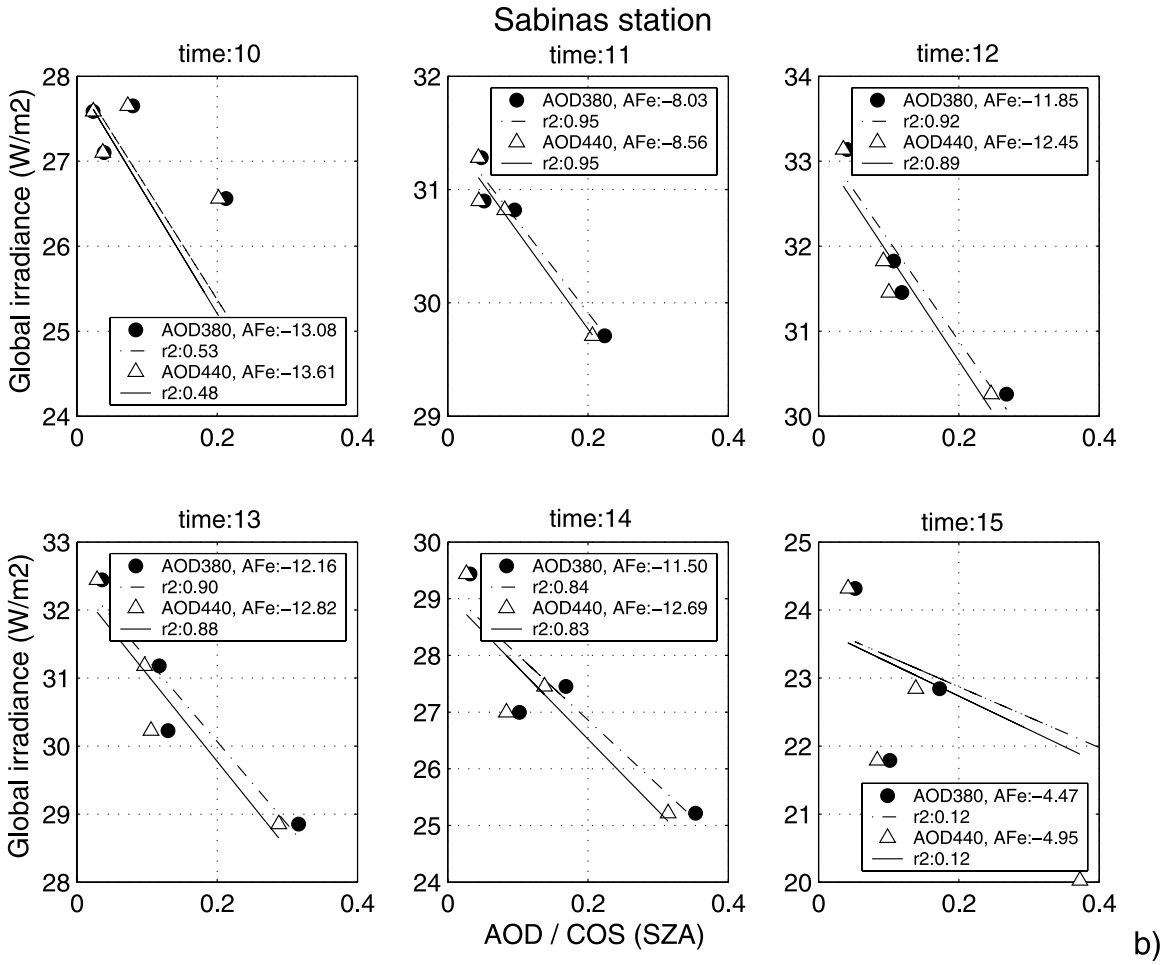

Figure 9. (continued)

dependent on the aerosol absorption extinction ratio, which can be expressed as $k = 0.1 + 2(1 - \omega) - 2(1 - \omega)^2 \pm 0.04$ (at $\theta = 30^\circ$ and $\lambda = 325$ nm) where ω is the single scattering albedo. We have found a k mean value of 0.30 ± 0.06, which agrees with the results obtained by *Krotkov et al.* [1998] for weakly absorbing aerosols. The C_T obtained ranges between 92–95% from the colocated irradiance and AOD (at 380 nm) measurements made at Armilla station between 10 and 17 July 2002. Also, the aerosol attenuation factor, η, was evaluated in this work to directly compare with literature. This magnitude can be defined by:

$$\eta(\lambda) = 1 - C_T(\lambda) \tag{6}$$

[25] Figure 10 shows this magnitude as a wavelength function, however, the spectral dependence is negligible. These results agree with the ones found by *Krotkov et al.* [1998]. These results show that under cloud free conditions atmospheric aerosols are an important source of uncertainty in retrieval UV radiation from satellite.

4. Conclusions

[26] A simultaneous calibration and intercomparison of seven UV spectroradiometers and six CIMEL Sun photometers was carried out during VELETA 2002 field campaign at Granada, Spain, between 8 and 19 July 2002. The analysis of the diurnal isentropic backward trajectories calculated at four different altitudes at the main station of the campaign, Armilla, shows that the dominant air masses originated in the North Atlantic Ocean and also in the north Iberian Peninsula, with the exception of the last 2 days in which the air masses approached from the Mediterranean Sea. The spectroradiometer intercomparison shows differences between them less than 4%, being this value reached for those without temperature control. In particular, the two instruments used to evaluate the aerosol forcing efficiencies presented a mean ratio of 1.000 ± 0.010. These results are quite good taking into account that the uncertainty in the UV measurement is around 5–6% [*WMO*, 1999]. With regards to the intercomparison of the AOD values, a deviation of less than 1.00 ± 0.01 was found to all channels being consistent with the results obtained by *Eck et al.* [1999].

[27] Once the quality of the measurement was guaranteed, aerosol radiative forcing efficiencies, ΔF_e, in the UV spectral region were calculated at two stations: Armilla and Sabinas, located within and outside the boundary layer, respectively. At Armilla the values of ΔF_e calculated at 380 nm fall within the range (-2.27, -10.44 W m$^{-2}/\tau$) at 380 nm and (-2.42, -11.76 W m$^{-2}/\tau$) at 440 nm; at Sabinas station the ΔF_e fall within the ranges (-3.35,

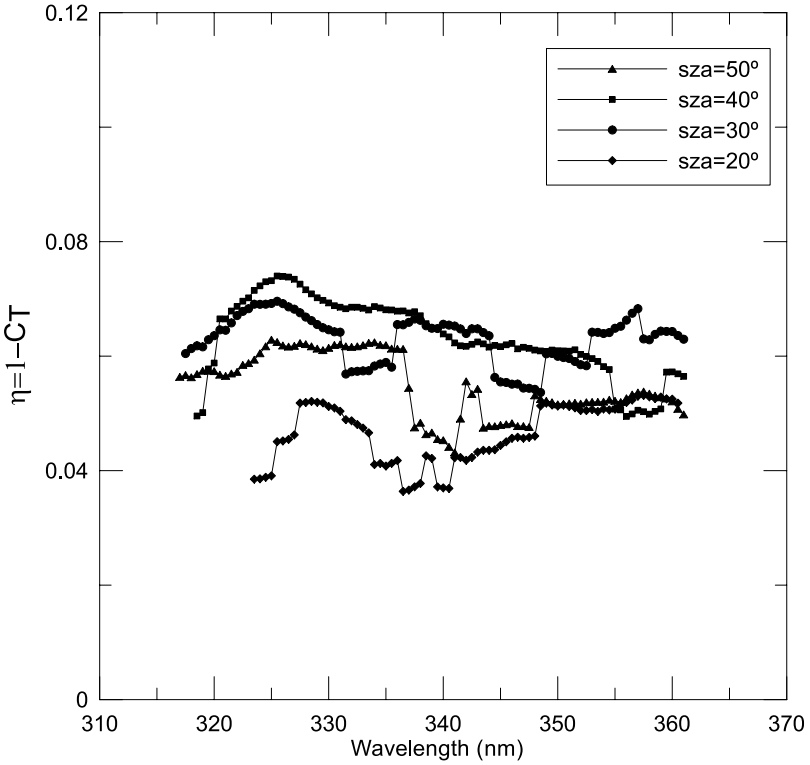

Figure 10. Aerosol attenuation factor in presence of weakly absorbing aerosols calculated at Armilla station.

-12.61 W m^{-2}/τ) and (-3.41, -13.60 W m^{-2}/τ) at 380 and 440 nm respectively. The correlation coefficient, r^2, of the method varies from 80% to 95% depending on the solar zenith angle. The fractional diurnal forcing efficiencies, ΔFDF_e, calculated at Armilla station were $-8.0 \pm 1.4\%/\tau_{380}$ and $-8.6 \pm 1.3\%/\tau_{440}$, and at Sabinas station $-12.0 \pm 2.3\%/\tau_{380}$ and $-12.6 \pm 2.3\%/\tau_{440}$.

[28] The dependence between the global irradiance and the aerosol optical depth was studied in order to experimentally obtain the aerosol transmittance factor, C_T, necessary to evaluate the surface UV irradiance retrievals by satellite. The average aerosol attenuation factor, η, inferred from C_T, was $6.0 \pm 2.0\%$ under the presence of weakly absorbing aerosols and cloud free conditions.

[29] **Acknowledgments.** This work was supported by CICYT–MCYT through the coordinated projects CGL2004-05984-C07-05 and CGL2005-03428-C04-02. We also want to acknowledge to the Armilla Air Base, Sierra Nevada National park and the Pitres and Motril city halls for their support to the development of this campaign. Finally, we acknowledge the AERONET team for the #109 instrument and its data availability. Thanks to EU INTERREG III B project CLIMAAT MAC/2.3/A3 for economical support.

References

Alados-Arboledas, L., et al. (2004), VELETA2002 field campaign a general overview, *Opt. Pur. Apl.*, *37*(3), 3271–3276.

Bush, B. C., and F. P. J. Valero (2003), Surface aerosol radiative forcing at Gosan during the ACE–Asia campaign, *J. Geophys. Res.*, *108*(D23), 8660, doi:10.1029/2002JD003233.

Charlson, R. J., J. Langner, H. Rodher, C. B. Loevy, and S. Warren (1991), Perturbation of Northern Hemisphere radiative balance by anthropogenic sulphate aerosol, *Tellus, Ser. A*, *43*, 152–163.

Conant, W. C., J. H. Seinfeld, J. Wang, G. R. Carmichael, Y. Tang, I. Uno, P. J. Flatau, K. M. Markowicz, and P. K. Quinn (2003), A model for the radiative forcing during ACE-Asia derived from CIRPAS Twin Otter and R/V Ronald *H. Brown data* and comparison with observations, *J. Geophys. Res.*, *108*(D23), 8661, doi:10.1029/2002JD003260.

Díaz, J. P., F. J. Expósito, C. J. Torres, F. Herrera, J. M. Prospero, and M. C. Romero (2001), Radiative properties of aerosols in Saharan dust outbreaks using ground–based and satellite data: Applications to radiative forcing, *J. Geophys. Res.*, *106*, 18,403–18,416.

Draxler, R. R., and G. D. Hess (1997), Description of the Hysplit4 modeling system, *NOAA Tech. Memo. ERL ARL–224*, 24 pp.

Eck, T. F., B. N. Holben, J. S. Reid, O. Dubovik, N. T. O'Neill, I. Slutsker, and S. Kinne (1999), Wavelength dependence of the optical depth of biomass burning, urban and desert dust aerosols, *J. Geophys. Res.*, *104*, 31,333–31,349.

Estellés, V., et al. (2006), Intercomparison of spectroradiometers and Sun photometers for the determination of the aerosol optical depth during the VELETA-2002 field campaign, *J. Geophys. Res.*, 111, D17207, doi:10.1029/2005JD006047.

Gardiner, B. G., and T. J. Martin (1997), On measuring and modelling ultraviolet spectral irradiance, in *IRS'96: Current Problems in Atmospheric Radiation, Proceedings of the International Radiation Symposium, Fairbanks, Alaska. 19–24 August 1996*, edited by W. L. Smith and K. Stamnes, pp. 917–920, Deepak, Hampton Va.

Gröbner, J., et al. (2004) Quality assurance of spectral solar UV measurements in Europe (QASUME), paper presented at XXth Quadrennial Ozone Symposium, Int. Ozone Comm., Kos, Greece, 1–8 June.

Hatzianastassiou, N., B. Katsoulis, and I. Vardavas (2004), Global distribution of aerosol direct radiative forcing in the ultraviolet and visible arising under clear skies, *Tellus, Ser. B*, *56*, 51–71.

Herman, J. R., N. Krotkov, E. Celarier, and D. Larko (1999), UV 380 nm reflectivity of the Earth's surface, clouds and aerosols, *J. Geophys. Res.*, *104*, 12,059–12,076.

Holben, B. N., et al. (1998), AERONET—A federated instrument network and data archive for aerosol characterization, *Remote Sens. Environ.*, *66*, 1–16.

Intergovernmental Panel of Climate Change (2001), *Climate Change 2001: The Scientific Basis*, edited by J. T. Hougthon et al., 881 pp., Cambridge Univ. Press, New York.

Jayaraman, A., D. Lubin, S. Ramachandran, V. Ramanathan, E. Woodbridge, W. D. Collins, and K. S. Zalpuri (1998), Direct observations of aerosol radiative forcing over the tropical Indian Ocean during the Janauary–February 1996 pre-INDOEX cruise, *J. Geophys. Res.*, *103*, 13,827–13,836.

Kerr, J. B. (1997), *Observed Dependencies of Atmospheric UV Radiation and Trends*, *NATO ASI Ser.*, *Ser. I*, vol. 52, edited by C. S. Zerefos and A. F. Bais, Springer, New York.

Krotkov, N. A., P. K. Bhartia, J. R. Herman, V. Fioletov, and J. Kerr (1998), Satellite estimation of spectral surface UV irradiance in the presence of tropospheric aerosols: 1. Cloud-free case, *J. Geophys Res.*, *103*, 8779–8793.

Krotkov, N. A., J. R. Herman, P. K. Bhartia, V. Fioletov, and Z. Ahmad (2001), Satellite estimation of spectral surface UV irradiance: 2. Effects of homogeneous clouds and snow, *J. Geophys Res.*, *106*, 11,743–11,759.

Rajev, K., and V. Ramanathan (2001), Direct observations of clear-sky aerosol radiative forcing from space during the Indian Ocean Experiment, *J. Geophys Res.*, *106*, 17,221–17,235.

Slaper, H., and T. Koskela (1997), Methodology of intercomparing spectral sky measurements, The Nordic intercomparison of Ultraviolet and total ozone instruments at Izaña, October 1996, final report, *Meteorol. Publ. 36*, edited by B. Kjeldstad and T. Koskela, Finn. Meteorol. Inst., Helsinki.

Slaper, H., H. A. J. M. Reinen, M. Blumthaler, M. Huber, and F. Kuik (1995), Comparing ground-level spectrally resolved solar UV measurements using various instruments: A technique resolving effects of wavelength shift and slit width, *Geophys. Res. Lett.*, *22*, 2721–2724.

Stammes, P., and R. Noordhoek (2002), OMI Algorithm Theoretical Basis Document, vol. III, *Tech. Rep. ATBD-OMI-03*, NASA Goddard Space Flight Cent., Greenbelt, Md.

Van Hoosier, M. E., (1996), The ATLAS-3 solar spectrum, U.S. Nav. Res. Lab., Washington, D. C. (Available at ftp://susim.nrl.navy.mil/pub/atlas3)

World Health Organization (1994), INTERSUN: UV report—Update on activities of the INTERSUN project, *Rep. WHO/EHG/94.18*, Off. of Global and Integrated Environ. Health, Geneva, Switzerland.

World Meteorological Organization (1999), Scientific assessment of ozone depletion: 1998, *Global Ozone Res. and Monit. Proj., Rep. 44*, Geneva, Switzerland.

World Meteorological Organization (2003), Scientific assessment of ozone depletion: 2002, *Global Ozone Res. Monit. Proj., Rep. 47*, 498 pp., Geneva, Switzerland.

L. Alados-Arboledas and F. J. Olmo, Grupo de Física de la Atmósfera, Universidad de Granada, E-18071 Granada, Spain.

V. Cachorro, Grupo de Óptica Atmosférica, Universidad de Valladolid, E-47071 Valladolid, Spain.

A. M. Díaz, J. P. Díaz, F. J. Expósito, and O. E. García, Departamento de Física, Universidad de la Laguna, E-38200 S/C de Tenerife, Spain.

T. Elias and A. M. Silva, Évora Geophysics Centre, University of Évora, P-7000 Évora, Portugal.

J. A. González, Departamento de Física, Universitat de Girona, E-17071 Girona, Spain.

H. Horvath, Experimental Physics Institute, University of Vienna, A-1010 Vienna, Austria.

A. Labajo, Instituto Nacional de Meteorología, Leonardo Prieto Castro, 8, C. Universitaria, E-28040 Madrid, Spain.

J. Lorente, Departamento de Astronomía i Meteorología, Universitat de Barcelona, E-08007 Barcelona, Spain.

J. A. Martínez-Lozano and M. P. Utrillas, Grupo de Radiación Solar, Universitat de València, E-46010 València, Spain.

M. Pujadas, Departamento de Impacto Ambiental de la Energía, Centro de Investigaciones Energéticas, Medioambientales y Tecnológicas, E-28040 Madrid, Spain.

J. A. Rodrigues, Centro de Física de Plasmas, Instituto Superior Tecnico of Lisbon, Av. Rovisco Pais, 1049-001 Lisbon, Portugal.

M. Sorribas and J. M. Vilaplana, Estacion de Sondeos Atmosféricos de El Arenosillo, Instituto Nacional de Técnica Aeroespacial, Ctra. Huelva, Matalascañas, Km. 33, E-21130 Huelva, Spain.